

The effectiveness of thin films in lieu of hyperbolic metamaterials in the near field

Owen D. Miller,¹ Steven G. Johnson,¹ and Alejandro W. Rodriguez²

¹*Department of Mathematics, Massachusetts Institute of Technology, Cambridge, MA 02139*

²*Department of Electrical Engineering, Princeton University, Princeton, NJ 08544*

We show that the near-field functionality of hyperbolic metamaterials (HMM), typically proposed for increasing the photonic local density of states (LDOS), can be achieved with thin metal films. Although HMMs have an infinite density of internally-propagating plane-wave states, the external coupling to nearby emitters is severely restricted. We show analytically that properly designed thin films, of thicknesses comparable to the metal size of a hyperbolic metamaterial, yield an LDOS as high as (if not higher than) that of HMMs. We illustrate these ideas by performing exact numerical computations of the LDOS of multilayer HMMs, along with their application to the problem of maximizing near-field heat transfer, to show that single-layer thin films are suitable replacements in both cases.

Near-field optics involves coupling of evanescent waves and holds great promise for applications ranging from fluorescent imaging [1–3] to thermophotovoltaic heat transfer [4, 5]. Evanescent waves from nearby radiative emitters can couple, for example, to plasmon modes at metal-dielectric interfaces [6], surface states in photonic crystals [7], and, as recently proposed, to a continuum of propagating modes in effective, anisotropic materials with hyperbolic dispersion [8, 9]. In this letter, we show that the local density of states (LDOS) near a hyperbolic metamaterial (HMM) [8, 10–13], even in the perfect effective-medium limit, is fundamentally no larger than the LDOS near thin metal films. Despite the HMM states being accessible for almost all high-wavevector waves, their coupling strength to near-field electric dipoles is only moderate. We show analytically that thin metal films, whose resonant waves couple very strongly at a small number of large-wavevector states, yield an equally large LDOS upon integration over wavevector. Moreover, the film thickness required to match the operational frequency of the HMM is of the same order of magnitude as the size of the metal within the HMM, such that the thin film is much easier to fabricate. Although we begin with an idealized asymptotic analysis to illustrate the basic physics, we confirm these conclusions with exact calculations of LDOS and heat transfer in realistic materials, obtaining comparable results for HMMs and thin films.

Hyperbolic metamaterials are periodic, metallodielectric composites with a unit cell size a much smaller than the wavelength, simplifying their electromagnetic response to that of a homogeneous medium [8, 10, 14]. Typical structures have one- or two-dimensional periodicity, yielding an anisotropic effective-permittivity tensor that, for certain materials and dimensions, has components ϵ_{\parallel} (surface-parallel) and ϵ_{\perp} with opposite signs ($\epsilon_{\parallel}\epsilon_{\perp} < 0$). Such a material has hyperbolic dispersion, leading to propagating plane wave modes with parallel wavevector larger than the free-space wavevector, i.e. $k_{\parallel} > \omega/c$, for frequency ω . They have excited great interest because of their potential to increase the local density of states (LDOS) [9, 11–24], e.g. for radiative-lifetime

engineering [15–20] and near-field heat transfer enhancement [9, 11, 21–23].

Previous works have explained the increase in the LDOS as arising from the hyperbolic ω - k dispersion relation, which implies an infinite density of states (DOS) at all frequencies for which $\epsilon_{\parallel}\epsilon_{\perp} < 0$. Typically [25], the proposed metamaterials exhibit orders of magnitude enhancements for the LDOS, or for radiative heat transfer, when compared to vacuum [13, 19], bulk metal [11, 15–18, 23], or blackbody [9, 11, 21–23] systems. We will show, however, that the increased LDOS in each case is not due to anisotropy, but rather to the reduction in resonant frequency that arises when the fraction of metal is reduced. As we show below, an effective metamaterial with *isotropic* $\epsilon \approx -1$, which achieves the resonance shift without anisotropy, is better than the ideal HMM with oppositely signed permittivity components. While such an isotropic metamaterial would likely require complex three-dimensional fabrication [26, 27], here we show that thin films, well-studied systems with resonance frequencies far below the bulk plasma frequency ω_p [28–35], exhibit the same near-field functionality as HMMs. A primary difference is the larger bandwidth provided by thin films; conversely, one could say that HMMs offer selectivity. However, selectivity is a general property of metamaterials [26, 27, 36, 37] and does not arise from hyperbolicity.

As a means for comparing the HMM to the thin film, we encapsulate the response of either structure in a scattering matrix $S(k_{\parallel}, \omega)$. Such a description is valid for any linear system with translational and rotational symmetry, including a media stack with many layers, an effective material with anisotropic permittivity, or a single thin film. Although the ultimate quantity of interest is the LDOS $\rho(z, \omega)$ at a point z near the interface, as in Ref. 21 we will define the weighted local density of states (WLDOS) $\rho(z, \omega, k_{\parallel})$ by $\rho(z, \omega) = \int \rho(z, \omega, k_{\parallel}) dk_{\parallel}$, thereby resolving the contribution at each k_{\parallel} . In the near field ($k_{\parallel} \sim 1/z \gg \omega/c$), the WLDOS of an electric dipole is dominated by contributions from the p (TM) polariza-

tion, given by [38, 39]:

$$\rho(k_{\parallel}, \omega, z) \approx \frac{1}{2\pi^2\omega} k_{\parallel}^2 e^{-2k_{\parallel}z} \text{Im} S_{21}(k_{\parallel}, \omega). \quad (1)$$

Regardless of the origin of the large-wavevector states, i.e. from either a continuum of propagating hyperbolic modes or a discrete set of plasmonic modes, the key to increasing the LDOS is to increase $\text{Im} S_{21}$, the imaginary part of the reflection coefficient. Thus, even if the DOS *within* a structure is infinite, as in an ideal HMM, the local density of states (LDOS) near the structure additionally requires strong external coupling. We will see that HMMs have only moderate external coupling, with $\text{Im} S_{21} \leq 1$, limiting their total LDOS.

Anisotropic permittivity and hyperbolic dispersion: To isolate the contribution of anisotropy, without any shift in resonance, we first compare the ideal anisotropic material, with hyperbolic dispersion, to the ideal isotropic metallic permittivity, which supports surface plasmon modes. We assume a single interface, with vacuum on one side and a bulk material on the other. Forgoing fabrication concerns for the moment, we ask what material provides the largest near-field LDOS at large parallel wavevector $k_{\parallel} \gg \omega/c$? A surface plasmon at a metal–vacuum interface exhibits maximum DOS for $\epsilon_{\text{metal}} = -1$ [40]. Similarly, the largest LDOS occurs for an HMM with $\epsilon_{\parallel} = -1$ and $\epsilon_{\perp} = 1$ [13, 21] (or vice versa, at large k_{\parallel} only the product matters and there is no distinction between Type I and Type II HMMs). We can add any amount of loss ϵ_i to the permittivities, defining the permittivities to be:

$$\epsilon_{\text{ideal metal}} = -1 + i\epsilon_i \quad (2)$$

$$\epsilon_{\text{ideal HMM}} = \begin{pmatrix} -1 & 0 & 0 \\ 0 & -1 & 0 \\ 0 & 0 & 1 \end{pmatrix} + i\epsilon_i \quad (3)$$

The imaginary parts of the (TM) reflectivity S_{21} for the ideal metal and HMM are

$$\text{Im}(S_{21})_{\text{ideal metal}} = \text{Im}\left(\frac{\epsilon - 1}{\epsilon + 1}\right) = \frac{2}{\epsilon_i} \quad (4)$$

$$\text{Im}(S_{21})_{\text{ideal HMM}} = \text{Im}\left(\frac{\epsilon_{\parallel}\epsilon_{\perp} - \sqrt{\epsilon_{\parallel}\epsilon_{\perp}}}{\epsilon_{\parallel}\epsilon_{\perp} + \sqrt{\epsilon_{\parallel}\epsilon_{\perp}}}\right) \quad (5)$$

$$= \frac{2\sqrt{1 + \epsilon_i^2}}{2 + \epsilon_i^2} \quad (6)$$

where the reflectivities are independent of k_{\parallel} in the limit $k_{\parallel} \gg \omega/c$. The ratio of the respective LDOS is then:

$$\frac{\rho_{\text{ideal metal}}(k_{\parallel}, \omega)}{\rho_{\text{ideal HMM}}(k_{\parallel}, \omega)} = \sqrt{1 + 1/\epsilon_i^2} + \frac{1}{\epsilon_i\sqrt{1 + \epsilon_i^2}} > 1 \quad (7)$$

where we see that regardless of the loss value, the ideal metal, with $\epsilon = -1 + i\epsilon_i$, is always better than the HMM

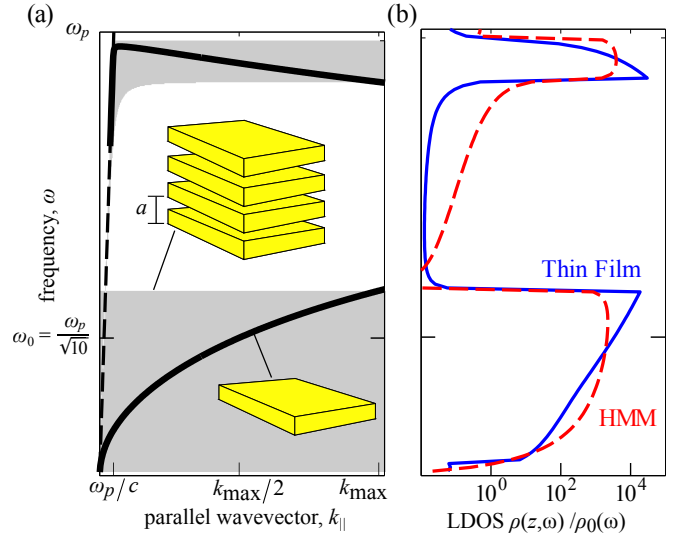


FIG. 1. (a) Comparison of the continuum of modes in an HMM to the discrete modes of a thin film. The surface modes of thin films have two branches, corresponding to symmetric and antisymmetric modes, that split away from $\omega_p/\sqrt{2}$. The HMM is designed for maximum LDOS at $\omega_0 = \omega_p/\sqrt{10}$, while the film is designed to have a resonance at $(\omega_0, k_{\text{max}}/2)$. The HMM comprises alternating layers of a lossless Drude metal (plasma frequency ω_p) and dielectric $\epsilon = 1$, with metallic fill fraction f given by Eq. (8). The thin film consists of the same metal, with thickness d given by Eq. (10). The unit cell $a = 0.1c/\omega_p$ ($k_{\text{max}}c/\omega_p = 20\pi$). HMMs exhibit $\text{Im}(S_{21}) \approx 1$ (shading indicates $\text{Im}(S_{21}) > 0$) for many k_{\parallel} , whereas thin films provide resonances with $\text{Im}(S_{21}) \gg 1$ for smaller bandwidths Δk_{\parallel} . (b) LDOS for each structure (normalized to the vacuum LDOS ρ_0) at $z = a$, the closest point at which EMT is valid. Note that the two structures have almost equal LDOS at ω_0 , as predicted by Eqs. (13,14).

with $\epsilon = (\epsilon_{\parallel}, \epsilon_{\perp}) = (-1, 1) + i\epsilon_i$. There should be no difference in photon lifetimes, as in each case the complex wavevector of either the surface plasmon or HMM mode is of the form $k_{\parallel} \approx [(1 + i)/\sqrt{2}\epsilon_i] \omega/c$. We note that the choice of permittivity in Eqs. (2,3) is exactly optimal only for $\epsilon_i = 0$, but that is true for both structures, and thus their relative performance is still meaningful. Moreover, in the exactly optimal limit as $\epsilon_i \rightarrow 0$, the metal's LDOS diverges, whereas the HMMs remains finite.

HMM vs. thin film: Away from the surface–plasmon frequency where $\epsilon \approx -1$, can metals still compete with HMMs? Bulk metals cannot, since their coupling to the single–interface surface plasmon is weak. Alternatively, it is well known that a thin metallic slab couples the front- and rear-surface plasmons [28–30, 40], yielding a symmetric mode that can exist at $\omega \ll \omega_p$ even for large k_{\parallel} . The thin film modes still asymptotically approach $\omega_p/\sqrt{2}$ as $k_{\parallel} \rightarrow \infty$, but if k_{max} is the maximum k_{\parallel} of interest—defined in HMMs by the unit cell—a film can exhibit low–frequency modes at $k_{\parallel} \sim k_{\text{max}}$.

For the thin metal film to be a practical replacement

for hyperbolic metamaterials, the optimal structure must not be too thin. We now analyze a second case: optimizing the near-field LDOS over a band of frequencies centered at ω_0 , for a lossless metal with permittivity $\epsilon(\omega_0) = \epsilon_m \ll -1$ (to contrast with the $\epsilon = -1$ case studied previously). We will design an optimal HMM and an optimal metallic thin film, and find that the LDOS of each is roughly equal.

We consider HMMs composed of a metal with permittivity ϵ_m and a dielectric with permittivity $\epsilon = 1$ (for simplicity), with a metallic fill fraction f . Typical effective-medium theory (EMT) approximations of HMMs assume multilayer slabs [21, 41] or periodic cylinders [10, 11, 41]. For either one, the optimal fill fraction is given by

$$f \approx \frac{2}{|\epsilon_m|}, \quad (8)$$

chosen to satisfy the ideal relation $\epsilon_{\parallel} \cdot \epsilon_{\perp} \approx -1$ at ω_0 . We now have the lossless version of the ideal scenario analyzed before, yielding the imaginary part of the reflectivity as

$$\text{Im}(S_{21})_{\text{HMM}} = 1, \quad (9)$$

in agreement with previously derived results [21]. Although Eq. (9) is independent of wavevector, ultimately a , the size of the unit cell within the HMM, limits the EMT approximation to $k \lesssim k_{\text{max}} = 2\pi/a$ (another limiting factor is $2\pi/z$), such that the bandwidth of the contribution to the LDOS is $\Delta k_{\parallel} \approx 2\pi/a$.

We can similarly derive the optimal thin film structure, comprising the same metal with permittivity ϵ_m , and thickness d . To roughly match the performance of the HMM, we design the thin film to have a mode at $\omega = \omega_0$ and $k_{\text{res,tf}} = k_{\text{max}}/2 = \pi/a$. In agreement with the choice of dielectric within the HMM, we assume vacuum at the rear surface of the film. The reflectivity of a thin film [42] is given by $S_{21} = r_{01} [1 - \exp(-k_{\parallel}d)] / [1 - r_{01}^2 \exp(-2k_{\parallel}d)]$, where r_{01} is the reflectivity at the air-metal interface. It follows that the optimal thickness is given by:

$$d = \frac{a}{\pi} \ln |r_{01}| \approx \frac{2a}{\pi |\epsilon_m|} \approx \frac{af}{\pi}, \quad (10)$$

which represents a pole in the reflectivity spectrum.

Hence, we see that the optimal thickness is within a factor π of af ; that is, it scales with the size of the metal in the HMM. In a multilayer HMM af is exactly the thickness of the individual metal layers, while in e.g. nanorod HMMs, af is the individual nanorod radius multiplied by the square root of the fill fraction. Because the thin film has approximately the thickness of the metal within a single unit cell, the thin film will have less or nearly equal absorptive losses as compared to the full HMM structure.

To compute the bandwidth for the thin film, we add a loss ϵ'' to the permittivity to avoid singular poles in the reflectivity, and then take the limit $\epsilon'' \rightarrow 0$. Since $k_{\parallel}d \ll 1$ (which follows from $\epsilon_m \ll -1$), we can approximate $\exp(-2k_{\parallel}d) \approx 1 - 2k_{\parallel}d$. On resonance, the imaginary part of the reflectivity is given by

$$\text{Im}(S_{21})_{\text{thin film}} = \frac{2}{\epsilon'' k_{\text{res,tf}} d} = \frac{|\epsilon_m|}{\epsilon''} \quad (11)$$

The full-width half-max bandwidth Δk_{\parallel} of $\text{Im} S_{21}$ is

$$\Delta k_{\parallel} \approx \frac{2\pi}{a} \frac{\epsilon''}{|\epsilon_m|}. \quad (12)$$

The LDOS at ω_0 requires a full integration of Eq. (1), but we can define a simpler “reflectivity–bandwidth” product to approximate the contribution of the reflectivity to the integral (verifying later the accuracy of the approximation). From Eqs. (9,11,12), valid in the limits $k_{\parallel} \gg \omega/c$ and $|\epsilon_m| \gg 1$, we have:

$$[\text{Im}(S_{21}) \Delta k_{\parallel}]_{\text{HMM}} \approx k_{\text{max}} = \frac{2\pi}{a} \quad (13)$$

$$[\text{Im}(S_{21}) \Delta k_{\parallel}]_{\text{thin film}} \approx \frac{2\pi}{a}. \quad (14)$$

Thus, given an optimal HMM, a thin film can be designed without further fabrication difficulty and with approximately equal increase in LDOS.

Figure 1 clarifies the similarities between HMMs and metallic thin films. A lossless Drude metal is employed for both an optimal HMM and an optimal thin film. The center frequency is $\omega_0 = \omega_p/\sqrt{10}$, and the unit cell a is chosen to be $a = 0.1c/\omega_p$. The HMM fill fraction and thin film thickness are chosen according to Eqs. (8,10). The multilayer EMT is used (a nanorod model only shifts the upper band of states downward). The computations are exact and do not include any of the high- k approximations utilized in the analysis. Although the underlying modes are very different—a continuum of propagating modes in HMMs versus discrete guided modes for thin films—their LDOSs near ω_0 are approximately equal.

Comparisons of LDOS and heat transfer: We now move from asymptotic analytical results, which reveal the underlying physics, to rigorous computations of the LDOS and near-field heat transfer characteristics for real material systems. We assume multilayer implementations of the HMMs, which enables us to use the exact Green’s functions [43] in both computations [44], using the numerically stable scattering–matrix formalism [45].

Figure 2 compares the near-field LDOS for an HMM comprising Ag/AlO₂ (similar to Ref. 41), with that of a thin silver film on an AlO₂ substrate. In the WLDOS plots, one observes the contrast between the relatively large number of weakly-coupled HMM modes and the single, strongly-coupled plasmonic mode of the film. The integrated LDOS at $\lambda = 545\text{nm}$ is shown in Fig. 2(c),

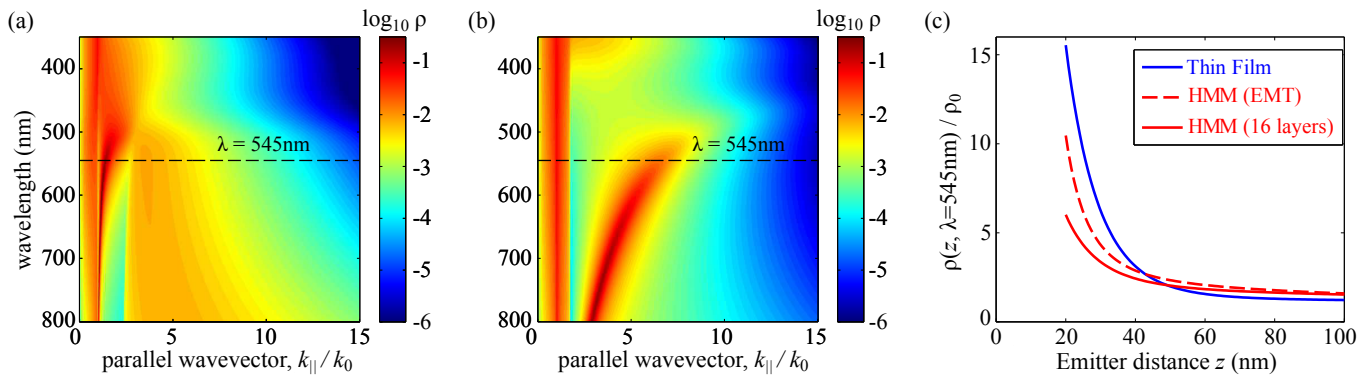


FIG. 2. (a,b) WLDOS computations ($z = 30\text{nm}$) for (a) Ag/AlO₂ HMM described by EMT and (b) Ag thin film on AlO₂ substrate, illustrating the distinct contrast between a continuum of propagating modes in the HMM and a single plasmonic mode in the film. For convenience, ρ is multiplied by ac , where c is the speed of light. (c) LDOS (normalized to the vacuum LDOS ρ_0) at $\lambda = 545\text{nm}$ for the thin film, the HMM (EMT), and a 16-layer implementation of the HMM ($a = 30\text{nm}$, $f = 0.4$).

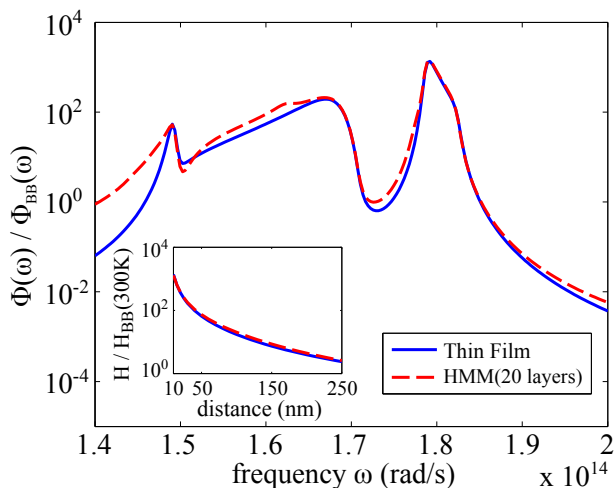


FIG. 3. Near-field heat transfer between SiC/SiO₂ structures. Heat flux spectrum for the HMM (red), comprising 20 layers (10 unit cells) with $a = 200\text{nm}$ and $f = 0.25$. Removing all but the top layer yields a SiC thin film of thickness 50nm on an SiO₂ substrate (blue). Each structure interacts with its mirror image, at a separation distance of 100nm. Inset: The total heat transfer, with one object at $T = 300\text{K}$ and the other at $T = 0\text{K}$.

which also includes a 16-layer implementation of the HMM, with a unit cell of 30nm and fill fraction $f = 0.4$ (chosen to approximately maximize the contribution of hyperbolic modes). The unit cell defines the minimum z at which EMT is applicable, no smaller than $z = 20\text{nm}$. One can see that the thin film (thickness = 8nm) has a larger LDOS in the near field.

Figure 3 compares the near-field heat transfer for a very different, but commonly proposed [9, 11, 21, 23, 34, 46, 47], material system: SiC/SiO₂. SiC is a phonon-polaritonic metal with negative permittivities for $\omega \in [1.5, 1.8] \times 10^{14}\text{Hz}$ ($\lambda \approx 11\text{--}12\mu\text{m}$), which is promising for heat-transfer applications where the peak of 300K

radiation is $\lambda \approx 7.6\mu\text{m}$. For the HMM we choose a 20 layer (10 unit cell) implementation with each 200nm unit cell consisting of 50nm of SiC and 150nm of SiO₂ ($\epsilon = 3.9$), consistent with previous work [9, 46]. The total heat transfer between objects at T_1 and T_2 is given by $H = \int_0^\infty d\omega [\Theta(\omega, T_1) - \Theta(\omega, T_2)] \Phi(\omega)$, where Φ is the temperature-independent flux spectrum and Θ is the mean energy per oscillator [48]. For comparison with the HMM, we also consider a thin film system. Instead of optimizing the thickness, we choose $d = 50\text{nm}$, such that the film is equivalent to removing 19 intermediate layers from the HMM, leaving only the top layer and the SiO₂ substrate. Each computation solves for the flux rate between an object and its mirror image. We see in Fig. 3 that the flux spectra for the HMM and the thin film are nearly identical at 100nm separation distance. The inset, the total heat transfer at $T_1 = 300\text{K}$ and $T_2 = 0\text{K}$, shows even greater similarity between the two. These computations show that not only is the thin film a suitable replacement for the HMM, but that the top layer of the HMM is primarily responsible for the heat transfer in the first place. A similar effect was observed in Ref. 46, albeit by labeling contributions within a structure rather than comparing two different ones. We arrive at a different conclusion than Ref. 46: rather than removing the top layer, to create a structure with less heat transfer but a greater relative contribution from propagating modes, we suggest simply replacing the HMM with a single thin layer, optimized for even greater heat transfer.

Conclusion: We have shown that thin films can operate as well or better than HMMs for increasing LDOS and heat transfer. Although previous works [41] have differentiated the “radiative” transitions of emitters near HMMs with “quenching” near a plasmonic metal, there is no fundamental difference between creating a photon in a bound thin-film guided mode, versus a high-wavevector photon that is trapped (propagating) within the HMM. For any amount of loss, the photon will eventually be

absorbed unless some other mechanism couples it to the far field, an equally difficult task for either structure. For any near-field application, then, we expect thin films to suffice as a replacement for HMMs. Away from the near field, of course, there are effects HMMs can exhibit that thin films cannot, such as negative refraction [49].

-
- [1] E. Betzig and J. K. Trautman, *Science* **257**, 189 (1992).
- [2] T. S. van Zanten, A. Cambi, M. Koopman, B. Joosten, C. G. Figdor, and M. F. Garcia-Parajo, *Proc. Natl. Acad. Sci. U. S. A.* **106**, 18557 (2009).
- [3] L. Schermelleh, R. Heintzmann, and H. Leonhardt, *J. Cell Biol.* **190**, 165 (2010).
- [4] M. Laroche, R. Carminati, and J.-J. Greffet, *J. Appl. Phys.* **100**, 063704 (2006).
- [5] S. Basu, Z. M. Zhang, and C. J. Fu, *Int. J. Energy Res.* **33**, 1203 (2009).
- [6] H. Morawitz and M. R. Philpott, *Phys. Rev. B* **10**, 4863 (1974).
- [7] C. Luo, S. G. Johnson, J. D. Joannopoulos, and J. B. Pendry, *Phys. Rev. B* **68**, 045115 (2003).
- [8] H. N. S. Krishnamoorthy, Z. Jacob, E. Narimanov, I. Kretzschmar, and V. M. Menon, *Science* **336**, 205 (2012).
- [9] Y. Guo and Z. Jacob, *Opt. Express* **21**, 15014 (2013).
- [10] J. Elser, R. Wangberg, V. A. Podolskiy, and E. E. Narimanov, *Appl. Phys. Lett.* **89**, 261102 (2006).
- [11] S.-A. Biehs, M. Tschikin, and P. Ben-Abdallah, *Phys. Rev. Lett.* **109**, 104301 (2012).
- [12] C. L. Cortes, W. Newman, S. Molesky, and Z. Jacob, *J. Opt.* **14**, 063001 (2012).
- [13] Y. Guo, W. Newman, C. L. Cortes, and Z. Jacob, *Adv. Optoelectron.* **2012**, 1 (2012).
- [14] A. Poddubny, I. Iorsh, P. Belov, and Y. Kivshar, *Nat. Photonics* **7**, 948 (2013).
- [15] Z. Jacob, J.-Y. Kim, G. V. Naik, a. Boltasseva, E. E. Narimanov, and V. M. Shalaev, *Appl. Phys. B* **100**, 215 (2010).
- [16] M. A. Noginov, H. Li, Y. A. Barnakov, D. Dryden, G. Nataraj, G. Zhu, C. E. Bonner, M. Mayy, Z. Jacob, and E. E. Narimanov, *Opt. Lett.* **35**, 1863 (2010).
- [17] O. Kidwai, S. V. Zhukovsky, and J. E. Sipe, *Opt. Lett.* **36**, 2530 (2011).
- [18] X. Ni, G. V. Naik, A. V. Kildishev, Y. Barnakov, A. Boltasseva, and V. M. Shalaev, *Appl. Phys. B* **103**, 553 (2011).
- [19] Z. Jacob, I. I. Smolyaninov, and E. E. Narimanov, *Appl. Phys. Lett.* **100**, 181105 (2012).
- [20] J. Kim, V. P. Drachev, Z. Jacob, G. V. Naik, A. Boltasseva, E. E. Narimanov, and V. M. Shalaev, *Opt. Express* **20**, 8100 (2012), arXiv:arXiv:0910.3981.
- [21] Y. Guo, C. L. Cortes, S. Molesky, and Z. Jacob, *Appl. Phys. Lett.* **101**, 131106 (2012).
- [22] E. E. Narimanov and I. I. Smolyaninov, in *Quantum Elec-*
- tron. Laser Sci. Conf.* (Optical Society of America, 2012).
- [23] B. Liu and S. Shen, *Phys. Rev. B* **87**, 115403 (2013).
- [24] D. Lu, J. J. Kan, E. E. Fullerton, and Z. Liu, *Nat. Nanotechnol.* **9**, 48 (2014).
- [25] one Pap. [12] there is a Comp. to a Ag thin Film. However, no Thick. is given, our own Comput. same Mater. with an Optim. Thick. yield a Larg. DOS thin Film than HMM.
- [26] J. B. Pendry, A. J. Holden, W. J. Stewart, and I. Youngs, *Phys. Rev. Lett.* **76**, 4773 (1996).
- [27] D. F. Sievenpiper, M. E. Sickmiller, and E. Yablonovitch, *Phys. Rev. Lett.* **76**, 2480 (1996).
- [28] E. N. Economou, *Phys. Rev.* **182**, 539 (1969).
- [29] K. L. Kliever and R. Fuchs, *Phys. Rev.* **153**, 498 (1967).
- [30] R. H. Ritchie, *Surf. Sci.* **34**, 1 (1973).
- [31] J. J. Burke, G. I. Stegeman, and T. Tamir, *Phys. Rev. B* **33**, 5186 (1986).
- [32] M. Francoeur, M. P. Menguc, and R. Vaillon, *Appl. Phys. Lett.* **93**, 043109 (2008).
- [33] S.-A. Biehs, D. Reddig, and M. Holthaus, *Eur. Phys. J. B* **55**, 237 (2007).
- [34] P. Ben-Abdallah, K. Joulain, J. Drevillon, and G. Domingues, *J. Appl. Phys.* **106**, 044306 (2009).
- [35] S. Basu and M. Francoeur, *Appl. Phys. Lett.* **98**, 243120 (2011).
- [36] D. Sievenpiper, L. Zhang, R. F. J. Broas, N. G. Alexopoulos, and E. Yablonovitch, *IEEE Trans. Microw. Theory Tech.* **47**, 2059 (1999).
- [37] S. J. Petersen, S. Basu, B. Raeymaekers, and M. Francoeur, *J. Quant. Spectrosc. Radiat. Transf.* **129**, 277 (2013).
- [38] F. Wijnands, J. B. Pendry, F. J. García-Vidal, P. M. Bell, P. J. Roberts, and L. Martín-Moreno, *Opt. Quantum Electron.* **29**, 199 (1997).
- [39] K. Joulain, R. Carminati, J.-P. Mulet, and J.-J. Greffet, *Phys. Rev. B* **68**, 245405 (2003).
- [40] S. A. Maier, *Plasmonics: Fundamentals and Applications* (Springer, 2007).
- [41] C. L. Cortes and Z. Jacob, *Phys. Rev. B* **88**, 045407 (2013).
- [42] L. A. Coldren, S. W. Corzine, and M. L. Mashanovitch, *Diode lasers and photonic integrated circuits* (Wiley, 2012).
- [43] J. E. Sipe, *J. Opt. Soc. Am. B.* **4**, 481 (1987).
- [44] Codes Free. available github.com/odmiller.
- [45] M. Francoeur, M. Pinar Mengüç, and R. Vaillon, *J. Quant. Spectrosc. Radiat. Transf.* **110**, 2002 (2009).
- [46] S.-A. Biehs, M. Tschikin, R. Messina, and P. Ben-Abdallah, *Appl. Phys. Lett.* **102**, 131106 (2013).
- [47] M. Francoeur, M. P. Mengüç, and R. Vaillon, *J. Phys. D. Appl. Phys.* **43**, 075501 (2010).
- [48] K. Joulain, J.-P. Mulet, F. Marquier, R. Carminati, and J.-J. Greffet, *Surf. Sci. Rep.* **57**, 59 (2005).
- [49] M. A. Noginov, Y. A. Barnakov, G. Zhu, T. Tumkur, H. Li, and E. E. Narimanov, *Appl. Phys. Lett.* **94**, 151105 (2009).